ACADEMIC PRESS

Available online at www.sciencedirect.com
SCIENCE DIRECT®

Journal of Solid State Chemistry 171 (2003) 57–68

JOURNAL OF SOLID STATE CHEMISTRY

http://elsevier.com/locate/jssc

The effect of varying the crystal structure on the magnetism, electronic structure and thermodynamics in the $Gd_5(Si_xGe_{1-x})_4$ system near $x=0.5$

V.K. Pecharsky,[a,b,*] G.D. Samolyuk,[a] V.P. Antropov,[a] A.O. Pecharsky,[a] and K.A. Gschneidner, Jr.[a,b]

[a] *Ames Laboratory, Iowa State University, Ames, IA 50011-3020, USA*
[b] *Department of Materials Science and Engineering, Iowa State University, Ames, IA 50011-3020, USA*

Received 12 June 2002; accepted 11 November 2002

Abstract

The crystal structure, magnetic and other physical properties of the intermetallic $Gd_5(Si_xGe_{1-x})_4$ phases are strongly dependent on the Si:Ge ratio (x). Especially intriguing behavior is observed when the chemical composition in this system is near $x \cong 0.5$, where small changes in the stoichiometry result in drastic variations in the chemical bonding, electronic structure, crystal structure, and magnetism. Furthermore, the fully reversible magnetic/crystallographic ($T_C \cong 270$ K) and the irreversible thermoelastic crystallographic (between ~ 500 and ~ 750 K) transformations exist near this critical chemical composition. Both of these transformations involve the same two crystallographic modifications: the monoclinic $Gd_5(Si_2Ge_2)$-type (β) and the orthorhombic Gd_5Si_4-type structures (α and γ). First principle calculations of the electronic structure and exchange coupling of these materials are in nearly quantitative agreement with the experiment. It appears that the unusual behavior observed in the near critical $Gd_5(Si_xGe_{1-x})_4$ phases is closely related to the stability of the well-defined sub-nanometer thick atomic slabs coupled with the flexibility of their arrangements.

1. Introduction

The 1967 discovery of the R_5Si_4 (R = Gd, Tb, Dy, Ho and Er) intermetallic phases [1] went just about unnoticed despite the presence of a conspicuous anomaly: the silicide—Gd_5Si_4—orders ferromagnetically at $T_C = 336$ K, which is nearly 40 K higher than that of the elemental Gd ($T_C = 294$ K). The abnormal increase in the Curie temperature of the crystalline material upon dilution of the magnetic Gd^{3+} sublattice by roughly the same amount of the non-magnetic silicon is especially intriguing because the seemingly isostructural germanide—Gd_5Ge_4—was classified as an antiferromagnet with $T_N = 15$ K. Thirty years later the reports about the giant magnetocaloric effect [2–4] and the understanding of the relationships between the room temperature crystal structures and chemical composition in the series of alloys in the $Gd_5(Si_xGe_{1-x})_4$ system [5] drew considerable attention to these and related intermetallic compounds [6–49].

Our knowledge of various $R_5(Si_xGe_{1-x})_4$ compounds, where R = rare earth metal, includes some exotic magnetic, electronic transport and thermodynamics properties, all of which are intimately related to similar but clearly diverse chemical bonding, electronic structure and crystallography of these complex metallic alloys [1–49]. The crystal and magnetic lattices in many of the $R_5(Si_xGe_{1-x})_4$ systems are coupled, and exhibit an extreme sensitivity to chemical composition, temperature, magnetic field and pressure. In many cases a distinctly non-linear response is triggered by a particular thermodynamic parameter exceeding a material-specific critical value. Thus near-critical regions are of special interest as they encompass states where minuscule variations in chemistry, temperature, magnetic field and/or pressure result in enormously large responses of both spin and lattice systems.

Especially intriguing is the fact that the replacement of silicon by its electronic twin—germanium—causes

*Corresponding author. Fax: 515-294-9579.
E-mail address: vitkp@ameslab.gov (V.K. Pecharsky).

0022-4596/03/$ - see front matter © 2002 Elsevier Science (USA). All rights reserved.
doi:10.1016/S0022-4596(02)00146-9

notable changes in the crystal structure and has a drastic influence on the physical properties of materials with the same R. Furthermore, strong magnetoelastic coupling observed when $R=$Gd, which is an S-state ion, is quite remarkable. In this work we describe our current understanding of the composition-structure-processing-property relationships in the $Gd_5(Si_xGe_{1-x})_4$ system in the near critical region ($x\cong 0.5$).

2. Crystallography of the $Gd_5(Si_xGe_{1-x})_4$ system

Crystal structures of alloys in the $Gd_5(Si_xGe_{1-x})_4$ system are complex and they contain a total of 36 atoms per unit cell, that are distributed among five to nine independent crystallographic sites in the orthorhombic and monoclinic crystal systems, respectively [5, 19]. Structurally, all of the $Gd_5(Si_xGe_{1-x})_4$ alloys are based on two different polyhedra, as shown in Fig 1: the cubooctahedron, [GdX_6Gd$_8$] (a), and the double trigonal prism, [X_2Gd$_8$] (b), where $X=$Si and Ge atoms that are nearly equably distributed among their respective crystallographic sites [19]. These two types of polyhedra are assembled into tightly bound, in effect two-dimensional slabs, which are shown in Figs 1c and d. Since both polyhedra are sharing four out of six rectangular faces, the chemical compositions of the slab fragments are ($Gd_3X_{10/3}$) and ($Gd_2X_{2/3}$) for the cubooctahedron and the coupled trigonal prisms, respectively. The chemical composition of the entire slab is $(Gd_5X_4)_\infty$ because there is one cubooctahedron for each double trigonal prism in the slab. In a way, the slab can be considered as a molecule that contains infinite number of atoms. The two distinctly different sites that are occupied by Si(Ge) atoms are indicated as $T1$ and $T2$: the former are located on the slab surface thus playing a role in the interlslab bonding, whereas the latter are found inside the slabs and contribute to the stability of the slabs.

The sub-nanometer-thick slabs (their total thickness along the b-axis is only $\sim$0.62 nm) are extremely stable and they can be found in practically every crystal structure known to exist in various $R_5(Si_xGe_{1-x})_4$ alloy systems, except for the silicon-rich La, Ce, Pr and Nd alloys [1, 16, 17, 19, 27, 35–37, 38, 40, 41]. The two crystal structures that are observed at $x\cong 0.5$ in the $Gd_5(Si_xGe_{1-x})_4$ system are shown in Fig. 2, and they are formed by a different arrangement of the nearly identical slabs. The first structure belongs to the orthorhombic Gd_5Si_4-type in which all slabs are interconnected via short X–X bonds (the interatomic distance, $\delta_{X-X}\cong 2.6$ Å). The second is the monoclinic $Gd_5Si_2Ge_2$-type structure, where the slabs are in fact identical to those found in the Gd_5Si_4-type structure but

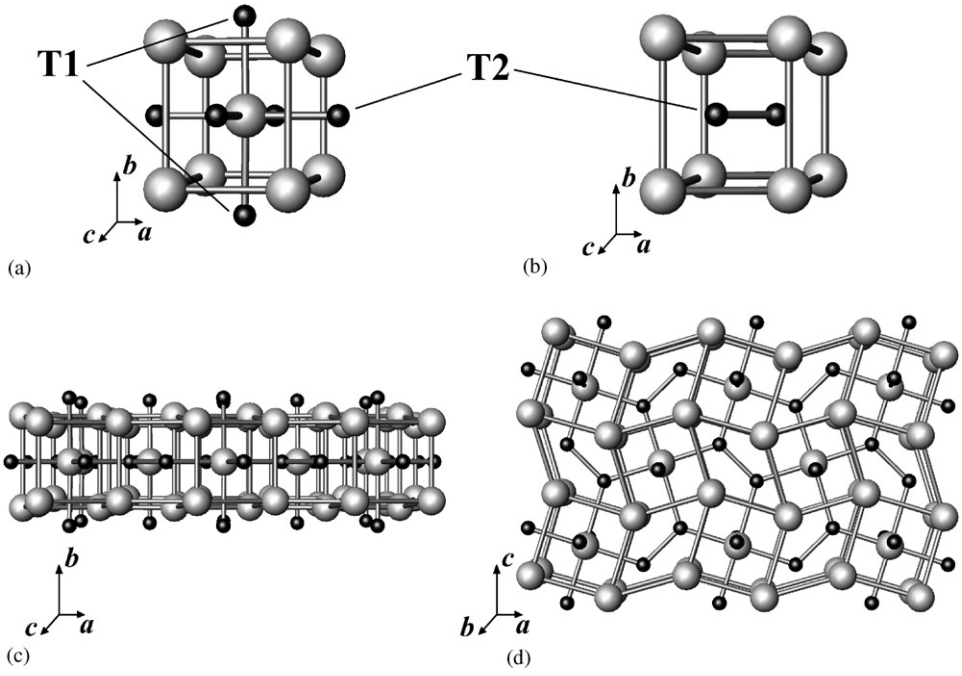

Fig. 1. The [RX_6] octahedron surrounded by the [R_8] cube (a) and double trigonal prism [X_2R_8] (b) as the building blocks of the $Gd_5(Si_xGe_{1-x})_4$ structures, where $R=$rare earth and $X=$Si and/or Ge atoms. The Si and/or Ge sites responsible for the interslab bonding are designated as $T1$, whereas the sites located inside the slabs are marked as $T2$. The two different projections of the slab formed by the two polyhedra are shown in (c) and (d). The full thickness of the slab along the b crystallographic direction is $\sim$6.2 Å and the slab is infinite along both the a and c crystallographic directions. Light gray large spheres indicate Gd atoms, while small black spheres are used to indicate both Si and Ge atoms nearly evenly mixed in the same lattice sites.

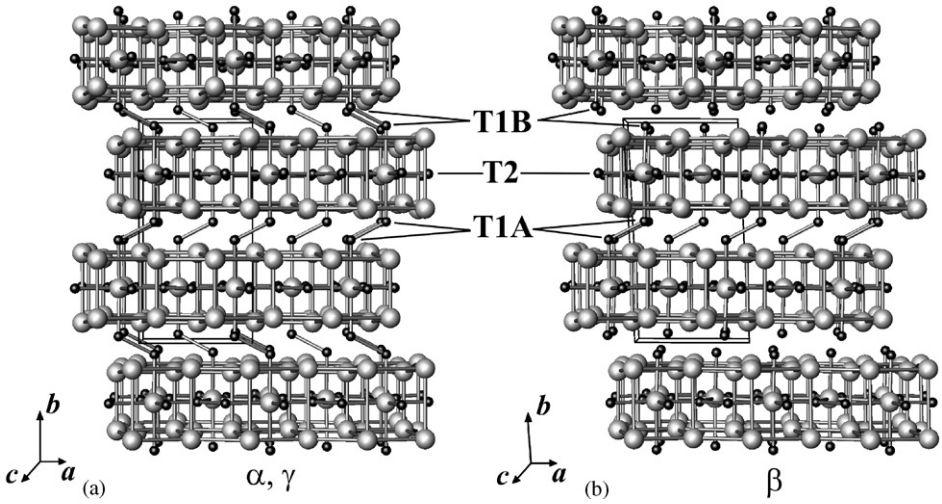

Fig. 2. The two crystal structures observed near the critical chemical composition at $x = 0.5$ in the $Gd_5(Si_xGe_{1-x})_4$ system: the orthorhombic, Gd_5Si_4—type (a), where all slabs are connected to one another with short Si(Ge)—Si(Ge) bonds, and the monoclinic, $Gd_5Si_2Ge_2$—type (b), where short Si(Ge)—Si(Ge) bonds are preserved between the pairs of slabs, while no such bonds exist between the pairs of the slabs. The orthorhombic structure is known to exist in both ferromagnetically ordered (α-phase) and paramagnetic (γ-phase) states. The monoclinic structure only exists in the paramagnetic state (β-phase). Notations ($T1$ and $T2$) used for the sites occupied by Si and Ge atoms are the same as in Fig. 1. The sites with short interslab bonds ($\delta_{X-X} = \sim 2.6$ Å) are designated as $T1$A, while the sites with no interslab bonds ($\delta_{X-X} = \sim 3.5$ Å) are marked as $T1$B. Gd and Si(Ge) atoms are indicated using large gray and small black spheres, respectively.

only pairs of slabs remain connected to one another. The short X–X bonds between the unconnected pairs are lost and the corresponding interatomic distance increases from ~ 2.6 to ~ 3.5 Å, while those of the connected pairs remain at ~ 2.6 Å.

The monoclinic $Gd_5Si_2Ge_2$-type structure is only stable in the paramagnetic state (the β-phase) in the composition range $\sim 0.38 \leqslant x \leqslant \sim 0.53$ (38). When the β-phase is cooled below its corresponding Curie temperature, which varies as a function of x, the coupled magnetic–crystallographic transition occurs, and the ferromagnetically ordered compounds always adopt the orthorhombic Gd_5Si_4-type structure—the α-phase [3, 5, 7, 8, 19, 20, 36, 38, 44]. This crystal structure change is illustrated in Fig. 3, which shows the difference in the powder diffraction patterns of the two crystallographic modifications of the alloy with $x = 0.5225$. The coupled magnetic–crystallographic transition is always complete and reversible at low temperatures, although it is characterized by a noticeable hysteresis. It is worth noting that the $\alpha \leftrightarrow \beta$ transition may also be triggered isothermally by magnetic field and/or pressure [8, 30].

The apparently identical crystallographic transformation can be decoupled from the magnetic ordering in alloys with $x \cong 0.5$. This is shown in Fig. 3, where the initially monoclinic paramagnetic $Gd_5(Si_{0.5225}Ge_{0.4775})_4$ phase (298 K) transforms into the orthorhombic Gd_5Si_4-type structure when heated to 690 K. The systematic shift of Bragg peaks to lower Bragg angles observed at 690 K when compared to their equivalents at 240 K is associated with thermal expansion of the lattice. Unlike the low-temperature magnetic–crystallographic transition ($\alpha \leftrightarrow \beta$), the high-temperature crystallographic-only transformation ($\beta \rightarrow \gamma$) is only triggered by temperature.

As established earlier [45], the $\beta \rightarrow \gamma$ transformation at $x = 0.5225$ is irreversible below ~ 730 K and the orthorhombic structure can be retained after cooling to room temperature. On the other hand, the monoclinic $Gd_5Si_2Ge_2$-type structure in this alloy can be restored by heat treatment at temperatures exceeding ~ 1200 K, i.e. the $\gamma \rightarrow \beta$ transformation occurs at high temperature. It appears therefore, that the monoclinic polymorphs of the $Gd_5(Si_{0.5225}Ge_{0.4775})_4$ and other alloys with $x \cong 0.5$ are high-temperature phases, which are in fact, metastable at room temperature. Despite their metastability, the monoclinic phases may exist indefinitely at room temperature and at any temperature, lower than the temperature at which $\beta \rightarrow \gamma$ transformations begin. For the $Gd_5(Si_{0.5225}Ge_{0.4775})_4$ composition the metastable (β) to stable (γ) transformation begins at ~ 500 K and it is nearly completed at ~ 730 K. As shown in Ref. [45], the $\beta \rightarrow \gamma$ transformation is thermoelastic, i.e. the fraction of the formed γ-phase remains constant as long as temperature remains constant.

3. Structure–property relationships in the $Gd_5(Si_xGe_{1-x})_4$ system near the critical composition, $x \cong 0.5$

It has been always implicitly assumed that the influence of the crystal structure of a material on its physical properties, especially magnetism (which is

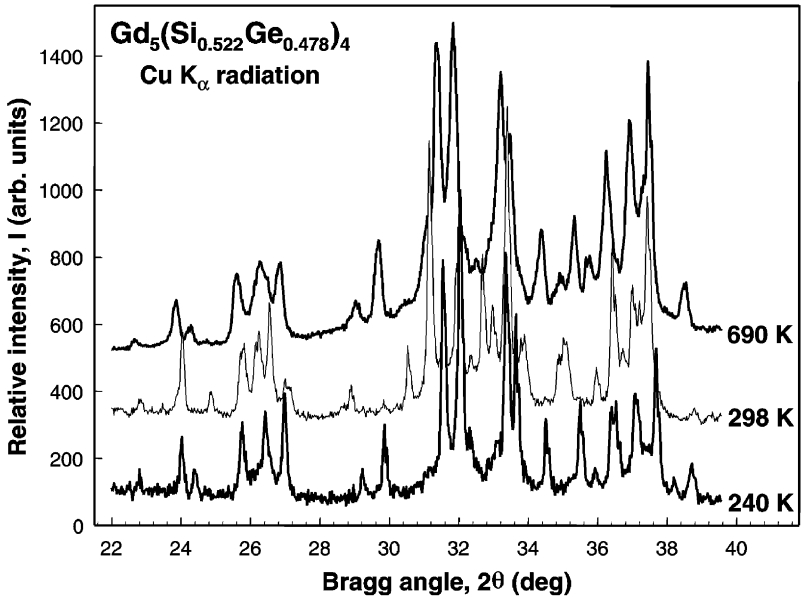

Fig. 3. The X-ray powder diffraction patterns of the monoclinic polymorph (β) of the $Gd_5(Si_{0.5225}Ge_{0.4775})_4$ compound at room temperature ($T = 298$ K, paramagnetic state), after cooling it to $T = 240$ K (ferromagnetic state), and after heating the sample to $T = 690$ K (paramagnetic state) indicating that both the low temperature (α) and the high temperature (γ) crystal structures are the same within the accuracy of the method. The temperatures shown in the figure are the actual temperatures at which powder diffraction experiments were carried out.

controlled by exchange interactions—a derivative of the interatomic distances and electronic structure), is immense. Unfortunately, it is more often true than not, that a material exists in a certain type of a crystal structure at a fixed chemistry and thus it is nearly impossible to experimentally examine the effects of varying the crystallography on the magnetism of a system with a constant stoichiometry. While theoretically it is possible to vary the crystal structure of the material and to predict the changes in the exchange interactions, the experimental verification of these predictions is generally unreliable, simply because the new crystal structure can only be obtained, if at all, by chemical substitutions. Thus, the question always remains: was the observed difference in properties due to the change in the structure of the material, or was it due to the chemical substitutions and thus the related changes of the electronic structures of the components, or was it due to the effects of both?

In this regard, the occurrence of two distinctly different types of crystal structures in a paramagnetic material (β- and γ-phase) without changing its chemical composition offers a unique opportunity not only to directly examine the effects of varying the crystal structure on the magnetism of the system, but also to verify and refine theoretical models. Indeed, the crystal structure of the $Gd_5(Si_xGe_{1-x})_4$ compounds has a pronounced effect on their magnetism:

- When the $Gd_5(Si_{0.5225}Ge_{0.4775})_4$ alloy adopts the monoclinic $Gd_5Si_2Ge_2$-type structure in the paramagnetic state (Fig. 2b), its properties clearly reflect the presence of the *first-order* coupled magnetic-crystallographic transformation at $T_C = 288$ K. The behavior of the magnetization as a function of magnetic field, shown in Fig. 4a, is indicative of a metamagnetic-like transition with the magnetic-field-induced transformation from a paramagnetic to a ferromagnetic state. This has been observed in several $Gd_5(Si_xGe_{1-x})_4$ alloys with the β-phase crystal structure [2–11, 30–35]. As noted above, the crystal structure of the ferromagnetically ordered $Gd_5(Si_{0.5225}Ge_{0.4775})_4$ compound is that of the Gd_5Si_4-type (Fig. 2a).
- When the same alloy has been transformed into the orthorhombic polymorph (γ) by heat treatment at ~ 750 K, the paramagnetic $Gd_5(Si_{0.5225}Ge_{0.4775})_4$ compound exists in the Gd_5Si_4-type structure. When cooled below its Curie temperature ($T_C = 302$ K, which is ~ 14 K higher than that of the monoclinic polymorph at the same chemical composition) this compound undergoes a *second-order* phase transition from a paramagnet to a ferromagnet. The behavior of the magnetization as a function of magnetic field has changed considerably, and it is similar to that of conventional ferromagnets (Fig. 4b).

A similar behavior has been observed for two other alloys ($x = 0.495$ and 0.5) in the $Gd_5(Si_xGe_{1-x})_4$ system, (Fig. 5). Both alloys were found to exist in two different modifications in the paramagnetic state—β and γ. When

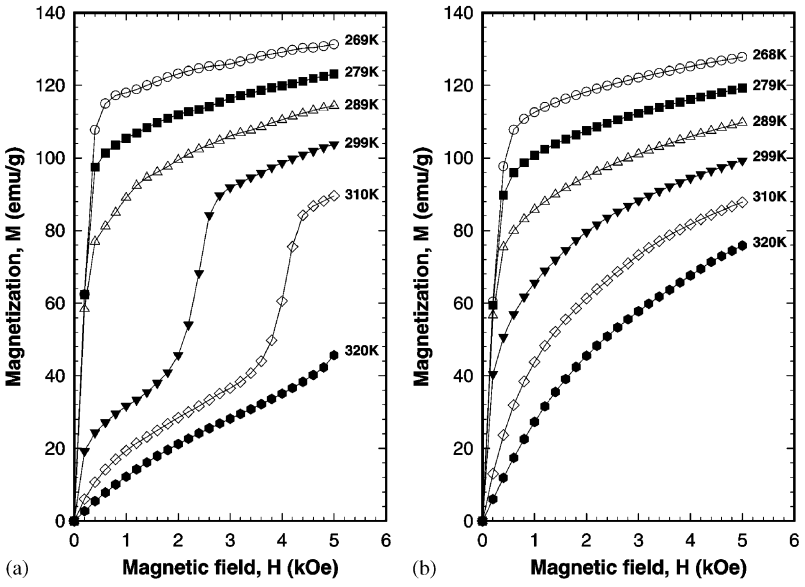

Fig. 4. The behavior of the magnetization as a function of magnetic field measured during field increase using a sample of the β monoclinic $Gd_5(Si_{0.5225}Ge_{0.4775})_4$ polymorph (a), and using a sample of the γ orthorhombic $Gd_5(Si_{0.5225}Ge_{0.4775})_4$ polymorph (b).

they adopt the monoclinic $Gd_5Si_2Ge_2$-type structure (β) in the paramagnetic state, the coupled magnetic-crystallographic transitions occur at notably lower temperatures when compared to the ferromagnetic-only ordering of the orthorhombic Gd_5Si_4-type polymorphs (γ) with the same chemical composition. The difference in the Curie temperatures of the two polymorphs increases linearly from 11 to 27 and 31 K when x varies from 0.5225 to 0.5 and 0.495, respectively. The trends in the Curie temperatures are identical to the trends established for the corresponding phases in the $Gd_5(Si_xGe_{1-x})_4$ system over a much broader range of concentrations [3, 20, 38]: the monoclinic polymorphs display strong concentration dependence of the Curie temperature as a function of composition from $\sim 0.38 \leqslant x \leqslant 0.53$, while the orthorhombic polymorphs have much weaker concentration dependence of T_C from $\sim 0.495 \leqslant x \leqslant 1$.

The crystal structures of the two polymorphs (β and γ) of the $Gd_5(Si_xGe_{1-x})_4$ compounds with $x \cong 0.5$ are formed by the practically identical slabs but are distinctly different in the interactions between the slabs (Fig. 2). Therefore, it is clear that the role of the interslab bonding on the magnetism in the $Gd_5(Si_xGe_{1-x})_4$ system is paramount, and it could be better understood by considering their electronic structure and magnetic properties from first principles. The results presented below were obtained using the tight-binding linear-muffin-tin-orbital approach [50] in the atomic sphere approximation (ASA) and the local density (LDA) approximation [51] with the spin–orbit (SO) coupling added variationally. Since it is well known that even the magnetic structure of the hexagonal close packed phase of Gd is not described properly in the LDA when 4*f* states are treated as valence states [52], the 4*f* states were treated as core states to avoid this uncertainty. The parameters of the exchange interactions were calculated as described in Ref. [53].

As shown schematically in the upper part of Fig. 6a, the interatomic distances between $X = Si(Ge)$ atoms which are responsible for the interslab bonding increase by ~ 0.9 Å during the transition from the α to the β-phase (19), also see Fig. 2. This dramatic change leads to a natural decrease of the corresponding bond strength and the lowering of the Fermi level. The relative stability of the orthorhombic polymorph in the ferromagnetically ordered state is associated with this shift of the Fermi level (E_F), which results in the smaller value of the effective magnetic exchange coupling, J_0, in the β-phase when compared to that in the α-phase as shown in Fig. 6b. Considering Helmholtz free energies of the two different polymorphs of $Gd_5(Si_xGe_{1-x})_4$ near $x = 0.5$, with such a modification of J_0, $F(T)_\alpha$ rises more rapidly with temperature when compared to $F(T)_\beta$, see Fig. 6c. Hence, the $Gd_5Si_2Ge_2$-type structure becomes stable at and above a critical temperature, T_m, where its free energy becomes lower than that of the Gd_5Si_4-type phase. The behavior of the two free energy functions in the vicinity of T_m results in a discontinuous change of the derivative, $[\partial F(T, P, H)/\partial T]_{P,H}$, and the magnetic–crystallographic transformation in the $Gd_5(Si_xGe_{1-x})_4$ system is thermodynamically a first-order phase transition when $x \cong 0.5$.

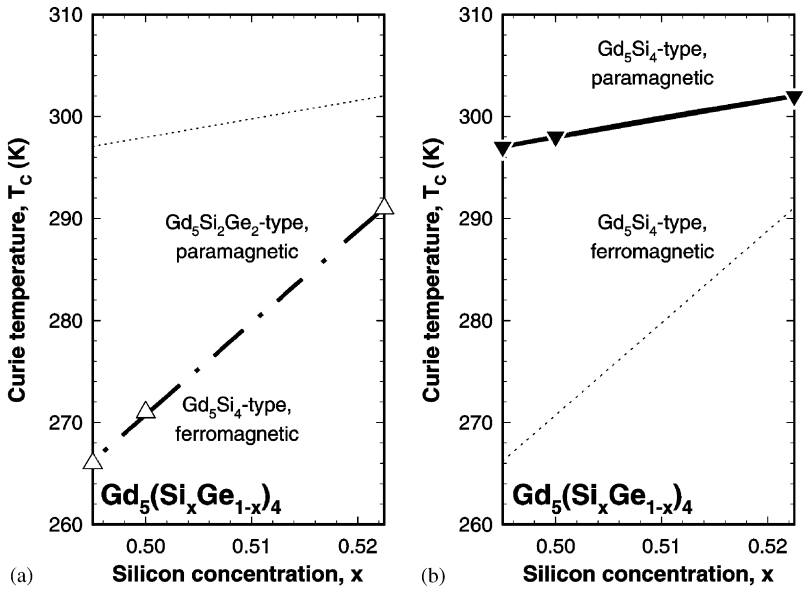

Fig. 5. The Curie temperature as a function of chemical composition in the $Gd_5(Si_xGe_{1-x})_4$ system for the metastable β monoclinic (a) and equilibrium γ orthorhombic (b) polymorphs near the critical composition, $x \cong 0.5$, as measured during heating. The dotted lines in each plot indicate the behavior of the Curie temperature of the second phase [γ in (a) and β in (b)]. The errors in the determination of the Curie temperature are comparable with the size of the data points.

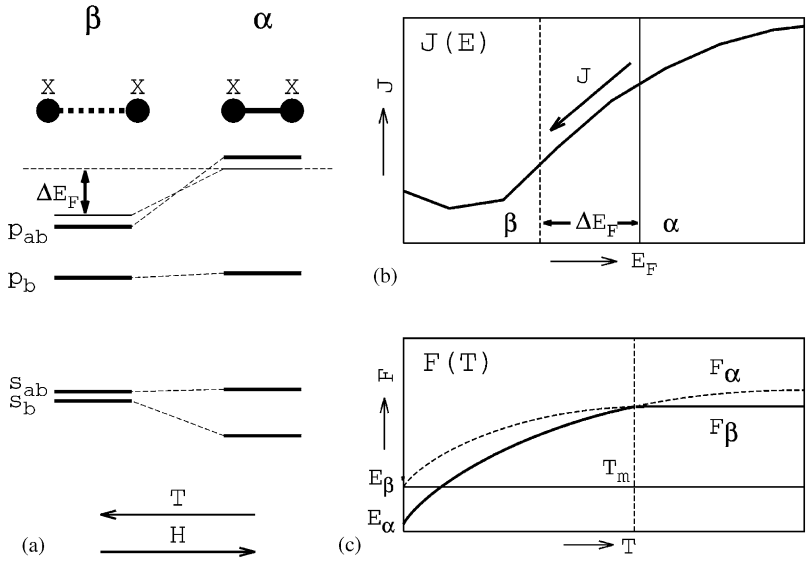

Fig. 6. The schematic of the coupled magnetic–crystallographic phase transition observed near $x = 0.5$ in the $Gd_5(Si_xGe_{1-x})_4$ system: (a) the structure of bonding (s_b and p_b) and antibonding (s_{ab} and p_{ab}) s and p states of X (Ge or Si) atoms responsible for the interslab bonding in the orthorhombic Gd_5Si_4-type (α) and its absence in the $Gd_5Si_2Ge_2$-type (β) phases with the corresponding shift (ΔE_F) of E_F in the $Gd_5Si_2Ge_2$-type phase; (b) the lowering of the effective magnetic exchange parameter, J_0, in the $Gd_5Si_2Ge_2$-type phase related to the shift of E_F; (c) the Helmholtz free energy, $F(T)$, as a function of temperature for both phases.

The total energy (TE) for the $Gd_5(Si_{0.5}Ge_{0.5})_4$ composition where Si and Ge atoms are nearly statistically disordered has been obtained by averaging the total energies for the two ordered structures (Fig. 7) with two possible distributions of atoms: in the first only Ge atoms occupy $T1$ positions and Si atoms are placed in $T2$ positions. In the second model, the site occupancy by Ge and Si is reversed. The calculated TE difference between the Gd_5Si_4-type and $Gd_5Si_2Ge_2$-type phases equals to 0.07 eV/unit cell or 22 K/atom. No energy barrier was found in these calculations. TE is sensitive to the specific ordering of Ge and Si atoms (Fig. 7), when the $T1$ sites are Ge-rich compared to the $T2$ sites, which are Ge-poor in both α- and β-phases. The latter is in good agreement with the experimental data [19].

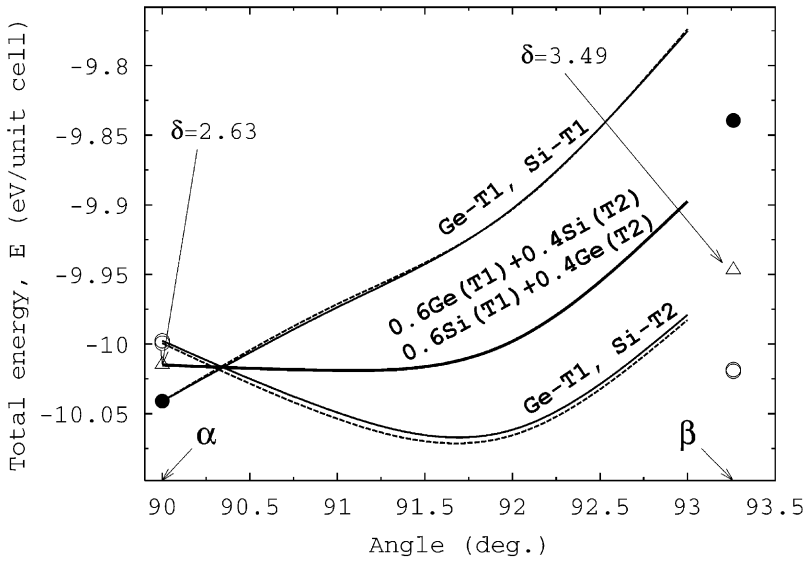

Fig. 7. The variation of TE during the Gd_5Si_4-type (α) to $Gd_5Si_2Ge_2$-type (β) transition of the FM $Gd_5(Si_{0.5}Ge_{0.5})_4$ compound assuming a linear transformation [56] of all atomic coordinates. The experimentally observed $T1$B–$T1$B distances (δ) are indicated in Å. The resulting theoretical $Gd_5Si_2Ge_2$-type structure is slightly different from that observed experimentally but this difference is small and does not affect any conclusions. The solid lines represent TE without SO coupling and the dashed lines show the same with SO coupling. The points correspond to TE of the experimentally observed crystal structures: two types of circles correspond to two types of Ge–Si ordering, whereas the average TE is shown by triangles. The middle solid line corresponds to TE assuming experimentally observed distribution of Ge and Si atoms in T' and T sites. The common shift due to SO coupling is not shown for simplicity.

Our analysis shows that the α-phase has lower TE when compared to the β-phase mainly due to the smaller one-electron energy ($E_{\rm bnd}$) of Ge(Si) atoms in the $T1$B positions since $E_{\rm bnd}$ of Ge(Si) atoms is strongly dependent on the $T1$B–$T1$B distance. Thus, to analyze the chemical bonding we use the following pair decomposition of $E_{\rm bnd}$:

$$\begin{aligned} E_{\rm bnd} &= \int^{E_{\rm F}} {\rm d}\varepsilon \sum_{RL}\sum_{R'L'} H_{RL,R'L'}N(\varepsilon)_{RL,R'L'} \\ &= \int^{E_{\rm F}} {\rm d}\varepsilon \sum_{RL}\sum_{R'L'} {\rm COHP}(\varepsilon)_{RL,R'L'} \\ &= \sum_{RL}\sum_{R'L'} {\rm ICOHP}_{RL,R'L'}, \end{aligned} \quad (1)$$

where $H_{RL,R'L'} \equiv \langle \chi_{RL}|\hat{H}|\chi_{R'L'}\rangle$ is a pair Hamiltonian; one electron wave function is a linear combination of atomic centered orbital χ_{RL} : $|\psi_j\rangle = \sum_{RL}|\chi_{RL}\rangle u_{RLj}$; $N(\varepsilon)_{RL,R'L'} = \sum_j u^*_{RLj}u_{R'L'j}\delta(\varepsilon_j - \varepsilon)$ is density of states (DOS) matrix; COHP is the crystal orbital Hamiltonian populations, and ICOHP is the integrated COHP [54].

The main contribution in the interslab bonds ($T1$–$T1$) comes from a pair of *sp* hybrid orbitals. These contributions have been extracted from the complete *s*-, *p*-, *d*- orbital basis set using an *sp* projection operator [54]. The *sp*-orbital for the each of the Ge atoms were constructed as 0.9 of *s*- plus *p*-orbital. The orbitals in the bond are centered on the neighboring Ge atoms and point towards each other along the connecting $T1$–$T1$ direction $[\vec{r} = (-0.15248,\ 0.05858,,0.29518)]$. The increase of one-half of $T1$–$T1$ (i.e., $T1$B–$T1$B) bond distances in the β-phase leads to the decrease of the corresponding elements of pair Hamiltonian $H_{RL',R'L}$. All contributions to $T1$B–$T1$B bond in the β-phase are smaller than in the α-phase (Fig. 8). The weakening of bond strength is accompanied by the modification of positions of bonding and anti-bonding states. The smaller value of H_{ss} produces smaller splitting between these *s* states. The decrease of H_{sp} elements also leads to a smaller splitting of *s* and *p* states. As a result the position of the antibonding *p* states in the β-phase is lowered as indicated by a large peak at -2.7 eV in Fig. 8b.

The analysis of pair contributions to the one-electron energy of Ge atom in $T1$B position shows that on-site value of ICOHP is similar in both structures (-18.39 and -18.29 eV in α- and β-phase, respectively). Hence, the decrease of $E_{\rm bnd}$ is related to a large negative contribution of the $T1$B–$T1$B bond in the α-phase. The total ICOHP value of the $T1$B–$T1$B bond is reduced from -1.9 eV in the α-phase to -0.14 eV in the β-phase. The total Ge T1B contribution to $E_{\rm bnd}$ is lowered from -23.15 eV in the α-phase to -21.83 eV in the β-phase. The total $\Delta E_{\rm bnd}$ ($T1$B) is equal to 1.33 eV, whereas the difference in $T1$B–$T1$B bond is 1.77 eV. The gain in $T1$B–$T1$B bond strength is partially compensated by the increase of Ge–Gd pair contributions in the β-phase. The lowering of *p* states leads to the appearance of two peaks below $E_{\rm F}$ in partial DOS of T1B Ge. This in turn increases the total number of states at these energies, lowering $E_{\rm F}$.

As it is shown in Fig. 7, the Gd_5Si_4-type$\rightarrow Gd_5Si_2Ge_2$-type crystallographic transformation is accompanied by the increase of TE for a ferromagnetically (FM) ordered $Gd_5(Si_{0.5}Ge_{0.5})_4$ when Ge atoms are distributed in $T2$ sites and Si atoms are placed in $T1$ sites. On the other hand, the total energy decreases when Ge is in $T1$ and Si is in $T2$, i.e. when Ge atoms are placed in $T1$B positions. The analysis of different contributions shows that the change of TE is dominated by the double-counted term (E_{dc}) of the valence electrons of Ge(Si) atoms in $T1$B sites, which is related to the fact that the wave functions of Ge atoms are more compact compared to those of Si and are less sensitive to the decrease of the muffin-tin sphere volume of $T1$B atoms in the β-phase.

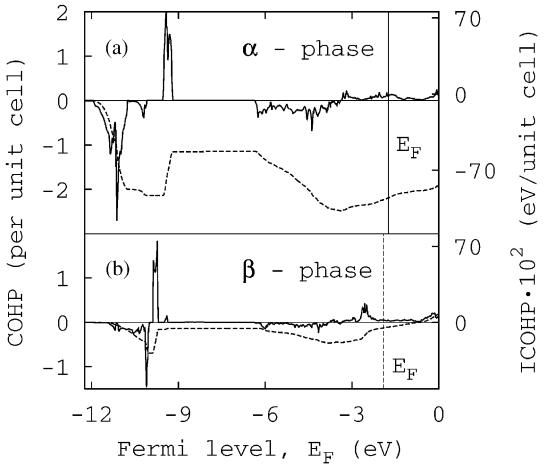

Fig. 8. The crystal orbital Hamiltonian populations (solid lines) and integrated crystal orbital Hamiltonian populations (dashed lines) of $T1$B–$T1$B Ge–Ge bond in the Gd_5Si_4-type (α) phase (a) and in the $Gd_5Si_2Ge_2$-type (β) phase (b) of the $Ge_5(Si_{0.5}Ge_{0.5})_4$ compound. The bottom of the band is placed at the same energy value for both phases. E_F are shown by vertical lines. Only the majority spin states are shown.

We also found that the pair exchange parameters J_{ij} are short ranged and do not exceed the unit cell size. The influence of E_F shift on the value of the effective exchange coupling parameter $[J_0(E_F) = \sum_j' J_{ij}]$ of Gd atoms located in the centers of cubooctahedra is illustrated in Fig. 9. It is worth noting that rigid band approximation works quite well in this case and the smaller value of $J_0(E_F)$ in the β-phase is simply determined by the shift of E_F.

The thermodynamics of phase transitions in $Gd_5(Si_xGe_{1-x})_4$ when $x \cong 0.5$ may be analyzed by calculating the free energy using Heisenberg model and mean field approximation (MFA) [55] based on the exchange parameters obtained as described above. The magneto-structural phase transition occurs when free energies of α- and β-phase become equal:

$$F_\alpha(T_m) = F_\beta(T_m), \tag{2}$$

where T_m is the temperature of the phase transition. The magnetic part of free energy can be written as

$$\begin{aligned} F(T) &= E_{FM} + F_{MF}(T) - F_{MF}(T=0), \\ F_{MF}(T) &= -T\sum_n \ln\left[\frac{\sinh(x_n)}{x_n}\right] + \sum_{n,m} J_{nm}^{(0)}\mu_n\mu_m, \\ x_n &= \frac{1}{T}(2\sum_m J_{nm}^{(0)}\mu_m + \mu_B M_n H), \\ F_{MF}(T=0) &= -\sum_n (J_n^{(0)} + \mu_B M_n H), \end{aligned} \tag{3}$$

where E_{FM} is the total energy of the ferromagnetic phase, $F_{MF}(T)$ is the free energy in the MFA (for $T > T_C$ $F_{MF}(T) = 0$, $\mu_n = \langle e_n^z \rangle$, where $\vec{e}_n = \vec{M}_n/|\vec{M}_n|$ corresponds to the direction of the atomic magnetic moments (M_n), n and m are the indices of non-equivalent magnetic atoms in the unit cell, and H is external magnetic field. The third term in the expression for $F(T)$

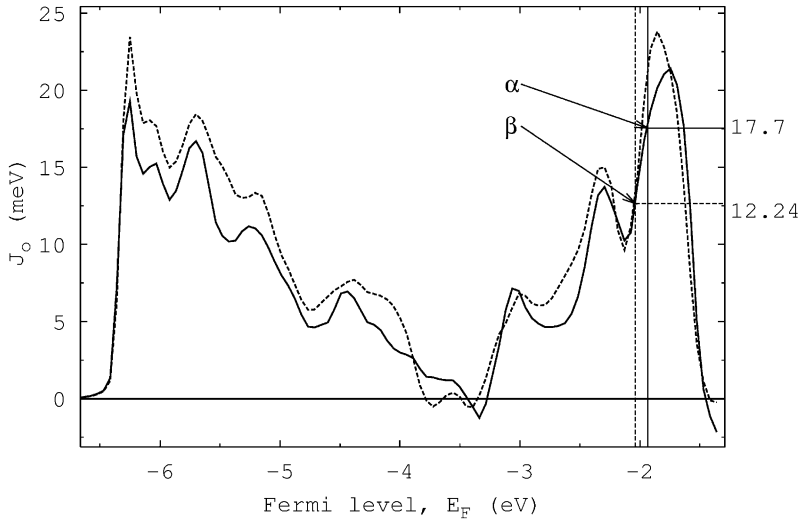

Fig. 9. Effective exchange coupling parameter, J_0, for Gd atoms located inside the cubooctahedra (see Fig. 1) as a function of E_F in the α (solid line)- and β (dashed line)-phase. The corresponding E_F are shown as solid and dashed lines for α and β phases, respectively.

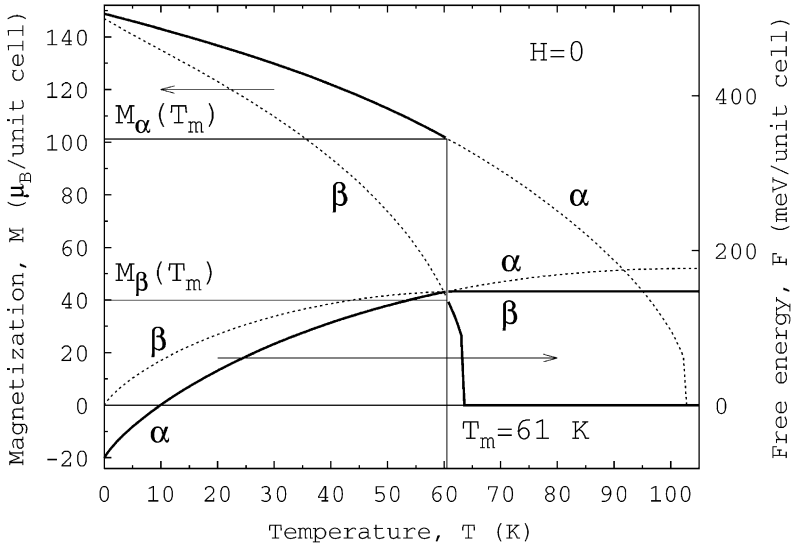

Fig. 10. Free energy (right-hand scale) and spontaneous magnetic moment (left-hand scale) of $Gd_5(Si_{0.5}Ge_{0.5})_4$ as functions of temperature in zero magnetic field. The metastable states (β-phase for $T<T_m$ and α-phase for $T>T_m$) are shown using dashed lines.

has been added to obtain a correct limit at zero temperatures $F(T=0)=E_{FM}$. The μ_n values were found from a system of non-linear equations

$$L(x_n)=\mu_n,$$
$$L(x)=\coth(x)-1/x, \quad (4)$$

where $L(x)$ is the Langeven function. This system of equations was solved iteratively.

Assuming that the crystal structure does not change, the magnetic system described in the MFA undergoes a second-order phase transition at various Curie temperatures, which depend on the type of the crystal structure of the compound. The value of the Curie temperature (T_c) was calculated as the largest solution of the system of equation

$$|T_{nm}-T\delta_{nm}|=0, \quad (5)$$

where $T_{nm}=2/3J_{nm}^{(0)}$, $\delta_{nm}=1$ for $n=m$ and 0 for $n\neq m$.

Thus, T_c calculated from Eq. (5) are 104 K for the Gd_5Si_4-type structure and 64 K for the $Gd_5Si_2Ge_2$-type structure. The T_m value is 61 K (Fig. 10) as established from Eq. 2. For $T<T_m$ the stable phase is the ferromagnetic α-phase. At $T=T_m$ it is replaced by the α-phase with a small spontaneous magnetization (we note that in the experiment this phase is the paramagnetic β-phase). Overall, the $Gd_5(Si_{0.5}Ge_{0.5})_4$ system undergoes a first-order magneto-structural phase transition at $T_m=61$ K with nearly a 60% reduction of the spontaneous magnetization relatively to its value at zero temperature. This result is in a quantitative agreement with the experimental data shown in Fig. 11. A sizeable disagreement of the calculated T_m (61 K) with the experimental value ($\sim$270 K) is related to both the underestimated magnetic exchange parameters and simplifications used in the description of the free energy, since we used the MFA for the magnetic part and did not include phonon and electronic contributions.

The influence of the applied magnetic field on the thermodynamics of the phase transition is illustrated in Fig. 12. In the presence of the magnetic field, the second-order magnetic phase transitions for the models with the same crystal structure vanish, which is evident from the absence of points where spontaneous magnetization is zero. As a result the free energy functions are increased less sharply with temperature compared to zero magnetic field and T_m is raised to 67 K for 23.5 kOe magnetic field. However, both the magnetization discontinuity and the first order nature of the magneto-structural transition are preserved. The calculated value of $dT_m/dH=0.26$ K/kOe is in a qualitative agreement with the observed values of $\sim$0.5–0.6 K/kOe, see Fig. 11.

4. Magnetic shape memory in the $Gd_5(Si_xGe_{1-x})_4$ system near $x=0.5$?

The coexistence of three phases in the $Gd_5(Si_xGe_{1-x})_4$ system when $x\cong0.5$, all observed at constant stoichiometry, i.e. the Gd_5Si_4-type ferromagnetically ordered α-phase, the $Gd_5Si_2Ge_2$-type paramagnetic β-phase and the Gd_5Si_4-type paramagnetic γ-phase brings about the following fundamental question: how can the same material adopt two different crystal structures in the paramagnetic state beginning with the same crystal structure in the ferromagnetic state? This question arises because all available experimental data indicate that when the orthorhombic, ferromagnetic Gd_5Si_4-type

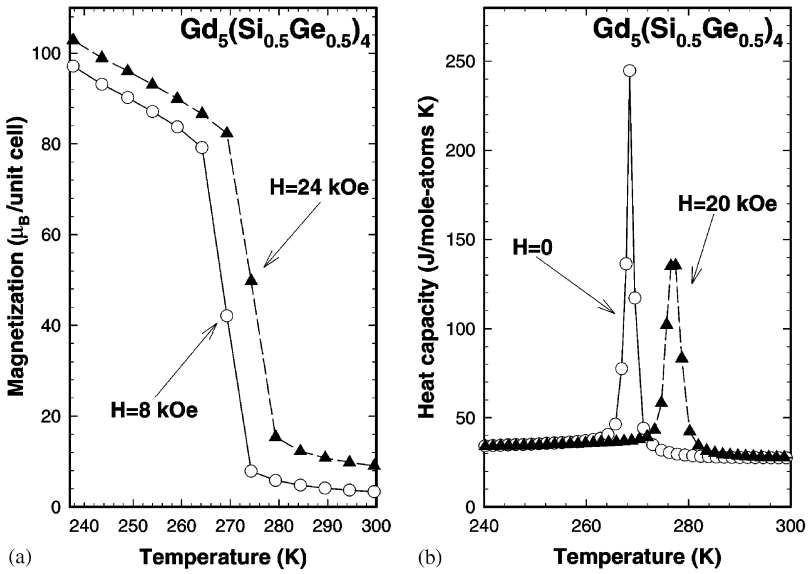

Fig. 11. The experimental behavior of the magnetization of $Gd_5(Si_{0.5}Ge_{0.5})_4$ in the lowest saturation magnetic field ($H=8$ kOe) and in 24 kOe magnetic field (a), and the heat capacity in zero and 20 kOe magnetic fields (b). Both the magnetization and heat capacity were measured during heating in a constant magnetic field.

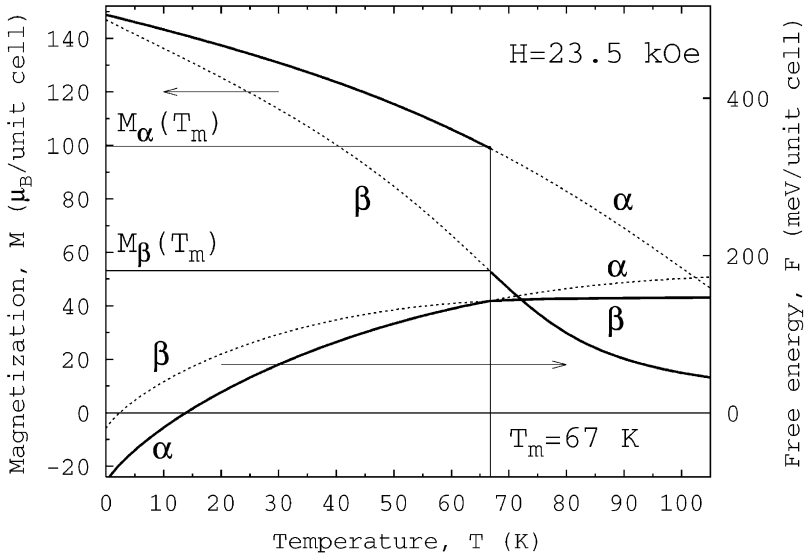

Fig. 12. Free energy (right-hand scale) and spontaneous magnetic moment (left-hand scale) of $Gd_5(Si_{0.5}Ge_{0.5})_4$ as functions of temperature in 23.5 kOe magnetic field. The metastable states (β-phase for $T<T_m$ and α-phase for $T>T_m$) are shown using dashed lines.

structure has been formed on cooling during the coupled magnetic-crystallographic transition from the paramagnetic monoclinic $Gd_5Si_2Ge_2$-type phase (e.g. Fig. 5), the magnetic disordering on heating is also accompanied by the orthorhombic-to-monoclinic crystal structure change [7, 8, 12, 19, 30]. On the other hand, when the orthorhombic ferromagnetic Gd_5Si_4-type structure has been formed during the simple magnetic ordering of the paramagnetic orthorhombic Gd_5Si_4-type phase (e.g. Fig. 5b), the magnetic disordering on heating occurs without the crystal structure change (see [45] and this work).

Given the complexity of the crystal structures and the limited resolution of X-ray powder diffraction data it appears that both the low- and high-temperature orthorhombic Gd_5Si_4-type phases are identical. Thus, in the absence of the more precise single-crystal data, collecting of which presents an extremely challenging experimental problem given the need for temperatures in excess of 700 K, it is easy to speculate that the material "remembers" its crystal structure in a paramagnetic state, in a way displaying a magnetic shape memory effect. However, if one recalls the sensitivity of the total energy of the $Gd_5(Si_{0.5}Ge_{0.5})_4$ to the distribution of Si

and Ge atoms between $T1$ and $T2$ sites, it is possible to analyze whether or not the deviation from the experimentally observed distribution (60% Ge in $T1$ and 40% Ge in $T2$) has any effect on the paramagnetic phase stability. Indeed, when the concentration of Ge in both $T1$ and $T2$ sites is set at 50%, the orthorhombic Gd_5Si_4-type phase becomes stable at all temperatures. Hence, it is reasonable to assume that the temperature induced $\beta \rightarrow \gamma$ crystallographic transformations is an order–disorder phase transition resulting in the completely statistical distribution of Si and Ge atoms between $T1$ and $T2$ sites during which all interslab bonds are restored. Similarly, the heat treatment of the γ-phase above ~ 1200 K likely results in the disorder–order phase transition and *in an enrichment of* $T1$ *sites with* Ge, thus stabilizing the β-phase in the paramagnetic state. This theoretical conclusion awaits its experimental verification.

Acknowledgments

The authors express their gratitude to Dr. E. Brück who raised the question about the possibility of the magnetic shape memory effect and with whom we had fruitful discussions of this phenomenon. We also are indebted to Drs. K.D. Belashchenko, L.S. Chumbley, B.N. Harmon, D.C. Jiles, T.A. Lograsso, G.J. Miller, J.E. Snyder and C. Stassis for continuing productive discussions related to many aspects of chemistry, materials science and physics of the title materials. The Ames Laboratory is operated by Iowa State University for the US Department of Energy (DOE) under Contract W-7405-ENG-82. This work was supported by the Office of Basic Energy Sciences, Materials Sciences Division of the US DOE.

References

[1] F. Holtzberg, R.J. Gambino, T.R. McGuire, J. Phys. Chem. Solids 28 (1967) 2283–2289.
[2] V.K. Pecharsky, K.A. Gschneidner Jr., Phys. Rev. Lett. 78 (1997) 4494–4497.
[3] V.K. Pecharsky, K.A. Gschneidner Jr., Appl. Phys. Lett. 70 (1997) 3299–3301.
[4] V.K. Pecharsky, K.A. Gschneidner Jr., J. Magn. Magn. Mater. 167 (1997) L179–L184.
[5] V.K. Pecharsky, K.A. Gschneidner Jr., J. Alloys Compd. 260 (1997) 98–106.
[6] V.K. Pecharsky, K.A. Gschneidner Jr., Adv. Cryogen. Eng. 43B (1998) 1729–1736.
[7] L. Morellon, P.A. Algarabel, M.R. Ibarra, J. Blasco, B. Garcia-Landa, Z. Arnold, F. Albertini, Phys. Rev. B 58 (1998) R14721–R14724.
[8] L. Morellon, J. Stankiewicz, B. Garcia-Landa, P.A. Algarabel, M.R. Ibarra, Appl. Phys. Lett. 73 (1998) 3462–3464.
[9] K.A. Gschneidner Jr., V.K. Pecharsky, J. Appl. Phys. 85 (1999) 5365–5368.
[10] J. Szade, G. Skorek, J. Magn. Magn. Mater. 196–197 (1999) 699–700.
[11] A. Giguere, M. Foldeaki, B. Ravi Gopal, R. Chahine, T.K. Bose, A. Frydman, J.A. Barclay, Phys. Rev. Lett. 83 (1999) 2262–2265.
[12] E.M. Levin, V.K. Pecharsky, K.A. Gschneidner Jr., Phys. Rev. B 60 (1999) 7993–7997.
[13] J. Szade, G. Skorek, A. Winiarski, J. Crystal Growth 205 (1999) 289–293.
[14] V.K. Pecharsky, K.A. Gschneidner Jr., J. Appl. Phys. 86 (1999) 6315–6321.
[15] E.M. Levin, V.K. Pecharsky, K.A. Gschneidner Jr., P. Tomlinson, J. Magn. Magn. Mater. 210 (1999) 181–188.
[16] G.H. Rao, J. Phys.: Condens Matter 12 (2000) L93–L99.
[17] K.A. Gschneidner, V.K. Pecharsky, A.O. Pecharsky, V.V. Ivtchenko, E.M. Levin, J. Alloys Compd. 303-304 (2000) 214–222.
[18] J. Stankiewicz, L. Morellon, P.A. Algarabel, M.R. Ibarra, Phys. Rev. B 61 (2000) 12651–12653.
[19] W. Choe, V.K. Pecharsky, A.O. Pecharsky, K.A. Gschneidner Jr., V.G. Young Jr., G.J. Miller, Phys. Rev. Lett. 84 (2000) 4617–4620.
[20] L. Morellon, J. Blasco, P.A. Algarabel, M.R. Ibarra, Phys. Rev. B 62 (2000) 1022–1026.
[21] V.V. Ivtchenko, V.K. Pecharsky, K.A. Gschneidner Jr., Adv. Cryogen. Eng. 46A (2000) 405–412.
[22] K.A. Gschneidner Jr., V.K. Pecharsky, E. Brück, H.G.M. Duijn, E.M. Levin, Phys. Rev. Lett. 85 (2000) 4190.
[23] J.R. Sun, F.X. Shu, B.G. Shen, Phys. Rev. Lett. 85 (2000) 4191.
[24] M. Foldeaki, R. Chahine, T.K. Bose, J.A. Barclay, Phys. Rev. Lett. 85 (2000) 4192.
[25] E.M. Levin, V.K. Pecharsky, K.A. Gschneidner Jr., Phys. Rev. B 62 (2000) R14625–R14628.
[26] K.A. Gschneidner Jr., A.O. Pecharsky, V.K. Pecharsky, T.A. Lograsso, D.L. Schlagel, in: R.G. Bautista, B. Mishra (Eds.), Rare Earths and Actinides: Science Technology and Applications IV The Minerals Metals & Materials Society, Warrendale, PA, 2000, pp. 63–72.
[27] Y.I. Spichkin, V.K. Pecharsky, K.A. Gschneidner Jr., J. Appl. Phys. 89 (2001) 1738–1745.
[28] E.M. Levin, A.O. Pecharsky, V.K. Pecharsky, K.A. Gschneidner Jr., Phys. Rev. B 63 (2001) 064426/1–064426/10.
[29] E.M. Levin, V.K. Pecharsky, K.A. Gschneidner Jr., Phys. Rev. B 63 (2001) 174110/1–174110/7.
[30] V.K. Pecharsky, K.A. Gschneidner Jr., Adv. Mater. 13 (2001) 683–686.
[31] E.M. Levin, K.A. Gschneidner, V.K. Pecharsky Jr., J. Magn. Magn. Mater. 231 (2001) 135–145.
[32] E.M. Levin, V.K. Pecharsky, K.A. Gschneidner Jr., G.J. Miller, Phys. Rev. B 64 (2001) 235103/1–235103/11.
[33] L. Morellon, P.A. Algarabel, C. Magen, M.R. Ibarra, J. Magn. Magn. Mater. 237 (2001) 119–123.
[34] L. Morellon, C. Magen, P.A. Algarabel, M.R. Ibarra, C. Ritter, Appl. Phys. Lett. 79 (2001) 1318–1320.
[35] R. Nirmala, V. Sankaranarayanan, K. Sethupathi, A.V. Morozkin, J. Alloys Compd. 326 (2001) 74–176.
[36] Q.L. Liu, G.H. Rao, H.F. Yang, J.K. Liang, J. Alloys Compd. 325 (2001) 50–53.
[37] Q.L. Liu, G.H. Rao, J.K. Liang, Rigaku J. 18 (2001) 46–50.
[38] A.O. Pecharsky, K.A. Gschneidner Jr., V.K. Pecharsky, C.E. Schindler, J. Alloys Compd. 338 (2002) 126–135.
[39] J.B. Sousa, M.E. Braga, F.C. Correia, F. Carpinteiro, L. Morellon, P.A. Algarabel, M.R. Ibarra, J. Appl. Phys. 91 (2002) 4457–4460.
[40] C. Ritter, L. Morellon, P.A. Algarabel, C. Magen, M.R. Ibarra, Phys. Rev. B 65 (2002) 094405/1–094405/10.

[41] H.F. Yang, G.H. Rao, W.G. Chu, G.Y. Liu, Z.W. Ouyang, J.K. Liang, J. Alloys Compd. 339 (2002) 189–194.
[42] O. Tegus, O. Dagula, E. Brück, L. Zhang, F.R. de Boer, K.H.J. Buschow, J. Appl. Phys. 91 (2002) 8534–8536.
[43] G.D. Samolyuk, V.P. Antropov, J. Appl. Phys. 91 (2002) 8540–8542.
[44] J. Leib, J.E. Snyder, C.C.H. Lo, J.A. Paulsen, P. Xi, D.C. Jiles, J. Appl. Phys. 91 (2002) 8852–8854.
[45] V.K. Pecharsky, A.O. Pecharsky, K.A. Gschneidner Jr., J. Alloys Compd. 344 (2002) 362–368.
[46] G. Skorek, J. Denisczcyk, J. Szade, J. Phys.: Condens. Matter 14 (2002) 7273–7386.
[47] B.N. Harmon, V.N. Antonov, J. Appl. Phys. 91 (2002) 9815–9820.
[48] J.S. Myeres, L.S. Chumbley, F. Laabs, A.O. Pecharsky, in: Processing and Fabrication of Advanced Materials X. Proceedings of the International Symposium on Processing Fabrication of Advanced Materials, Indianapolis, IN, November 5–8, 2001 (2002), pp. 110–120.
[49] B. Teng, M. Tu, Y. Chen, J. Tang, J. Phys.: Condens. Matter 14 (2002) 6501–6507.
[50] O.K. Andersen, O. Jepsen, Phys. Rev. Lett. 53 (1983) 2571–2574.
[51] U. von Barth, L. Hedin, J. Phys. C 5 (1972) 1629–1642.
[52] B.N. Harmon, V.P. Antropov, A.I. Liechtenstein, I.V. Solovyev, V.I. Anisimov, J. Phys. Chem. Solids 56 (1995) 1521–1524.
[53] M. van Schilfgaarde, V.P. Antropov, J. Appl. Phys. 85 (1999) 4827–4829.
[54] R. Dronskowski, P.E. Blochl, J. Phys. Chem. 97 (1993) 8617–8624.
[55] J.W. Negele, H. Orland, *Quantum Many-Particle Systems*, Advanced Book Program, Preseus Book, Massachusetts, 1998.
[56] W. Choe, G.J. Miller, Private communication.